



## OPEN ACCESS

## EDITED BY

Sathishkumar Kuppusamy,  
Bharathidasan University, India

## REVIEWED BY

Lizie Daniela Tentler Prola,  
Research Associate ISEST, United States  
Hosimin Selvaraj,  
Bharathidasan University, India

## \*CORRESPONDENCE

Zafar Hussain Ibupoto,  
✉ zaffar.ibhupoto@usindh.edu.pk

RECEIVED 26 March 2024

ACCEPTED 07 May 2024

PUBLISHED 04 June 2024

## CITATION

Bhatti MA, Dawi E, Tahira A, Hulio AA,  
Halepoto IA, Chang SA, Solangi AG, Nafady A,  
Tonezzer M, Haj Ismail AAK and Ibupoto ZH  
(2024), UV photodegradation of methylene  
blue using microstructural carbon materials  
derived from *Citrullus colocynthis*.  
*Front. Mater.* 11:1407485.  
doi: 10.3389/fmats.2024.1407485

## COPYRIGHT

© 2024 Bhatti, Dawi, Tahira, Hulio, Halepoto,  
Chang, Solangi, Nafady, Tonezzer, Haj Ismail  
and Ibupoto. This is an open-access article  
distributed under the terms of the [Creative  
Commons Attribution License \(CC BY\)](#). The  
use, distribution or reproduction in other  
forums is permitted, provided the original  
author(s) and the copyright owner(s) are  
credited and that the original publication in  
this journal is cited, in accordance with  
accepted academic practice. No use,  
distribution or reproduction is permitted  
which does not comply with these terms.

# UV photodegradation of methylene blue using microstructural carbon materials derived from *Citrullus colocynthis*

Muhammad Ali Bhatti<sup>1</sup>, Elmuez Dawi<sup>2</sup>, Aneela Tahira<sup>3</sup>,  
Ahmed Ali Hulio<sup>4</sup>, Imran Ali Halepoto<sup>5</sup>, Sajjad Ali Chang<sup>6</sup>,  
Abdul Ghaffar Solangi<sup>3</sup>, Ayman Nafady<sup>7</sup>, Matteo Tonezzer<sup>8</sup>,  
Abd Al Karim Haj Ismail<sup>2</sup> and Zafar Hussain Ibupoto<sup>4\*</sup>

<sup>1</sup>Centre for Environmental Sciences, University of Sindh Jamshoro, Jamshoro, Pakistan, <sup>2</sup>College of Humanities and Sciences, Ajman University, Department of Mathematics and Sciences, Ajman, United Arab Emirates, <sup>3</sup>Institute of Chemistry, Shah Abdul Latif University Khairpur Mirs, Khairpur, Pakistan, <sup>4</sup>Institute of Chemistry, University of Sindh, Jamshoro, Pakistan, <sup>5</sup>Institute of Physics, University of Sindh, Jamshoro, Pakistan, <sup>6</sup>National Centre of Excellence in Analytical Chemistry, University of Sindh Jamshoro, Jamshoro, Pakistan, <sup>7</sup>Department of Chemistry, College of Science, King Saud University, Riyadh, Saudi Arabia, <sup>8</sup>Department of Chemical and Geological Sciences, University of Cagliari, Monserrato, Italy

A low temperature aqueous growth followed by mild pyrolysis was used in this study to synthesize high-quality carbonized materials from the deserted plant *Citrullus Colocynthis*. It was found that the carbon material prepared for this study contained an abundance of functional groups and surface active sites. A few microns were evidently the size of the carbon material. This study investigated a variety of photocatalytic performance evaluation parameters, including initial dye concentration of methylene blue, pH effect on dye solution, scavenger stability, and recycle stability via irradiating UV light. Methylene blue degradation was found to be significantly affected by pH and concentration of the dye solution. It has been found that pH five is the most effective pH for the removal of dyes. As a result of the study, we found that methylene blue decays according to pseudo first order kinetics and is estimated to remove dye at an almost 100% rate.

## KEYWORDS

carbon material, *Citrullus colocynthis*, mild pyrolysis, methylene blue, photodegradation

## 1 Introduction

It has been well documented that dyes are widely used in numerous industries, including the dyeing of wool, cotton, fabrics, coloring papers, and redox reaction indicators (Panagopoulos, 2022a; Panagopoulos, 2022b; Panagopoulos, 2022a; Panagopoulos and Giannika, 2022). In contrast, dyes, such as methylene blue (MB), have been found to be highly carcinogenic and toxic to both animals and aquatic life. MB can cause permanent loss of vision and severe nerve damage when it is inhaled into the body. The development of cutting-edge methods that remove pollutants from wastewater in an efficient manner is therefore highly desirable. To address

this issue, different approaches have been developed that can degrade or remove pollutants, particularly dyes, from water bodies. It has been well documented in the literature that these approaches are effective. These include adsorption (Karimifard, and Moghaddam, 2018; Katheresan et al., 2018), chemical reduction (Katheresan et al., 2018), membrane filtration (Peng, and Guo, 2020), photocatalytic oxidation, catalytic ozonation, biological, ion exchange, and coagulation/fluctuation (Peng, and Guo, 2020), and their widespread application has been demonstrated in the literature. Catalytic degradation and adsorption are the most common methods used to remove dyes. A number of advantages distinguish photocatalytic oxidation of dyes from other methods, including the use of renewable energy (sunlight), ease of operation, high efficiency, and complete mineralization of dyes (Panagopoulos, 2022a; Panagopoulos, 2022b; Panagopoulos, 2022a). Photocatalytic processes have recently been improved by using nanomaterials, in particular carbon-based materials. Passivation of carbon based materials through functionalization has been demonstrated to modify and manipulate their complex structure, resulting in significantly improved catalytic properties. Graphene is a nanostructured carbon with unique properties such as high conductivity, adsorption, photocatalysis, photostability, co-catalysis, and photosensitizing properties. The Humer's method and its modified forms (Olak-Kucharczyk et al., 2020) are extremely popular methods for synthesizing graphene (Gu, et al., 2020). As an oxygenated version of graphene, graphene oxide (GO) is known as an oxygenated version of graphene. Reduced graphene oxide (rGO) is an alternative substitute for graphene since it contains fewer functional groups than graphene. In photocatalyst design, rGO acts as a supporting material because of its high electrical conductivity. As a result, rGO was combined with metal oxides in the development of composites in order to enhance their photocatalytic activity. Incorporating rGO into ZnO has been shown to improve its photocatalytic activity (Qin et al., 2017; Zhao et al., 2017). Furthermore, carbon quantum dots have been investigated for the removal of dye and have shown outstanding results. In conjunction with carbon quantum dots, composite systems have been devised to evaluate dye adsorption capacity (Yang et al., 2012; Velasco et al., 2013; Zhang et al., 2016; Sun et al., 2017; Cong and Zhao, 2018; Chen et al., 2020; Feng et al., 2020; Nasir et al., 2020; Shahib et al., 2022). *In situ* growth of metal oxides with hexagonal structures, such as ZnO, TiO<sub>2</sub> and carbon quantum dots, can be achieved using the hexagonal structure of graphite. In recent years, hybrid systems based on graphite semiconducting have been demonstrated to provide improved photocatalytic performance. Carbon quantum dots with a low dimension and a large surface area that exhibit an enriched active site at the surface that allows photogenerated reactive species to interact with dye molecules efficiently (Sudhaik et al., 2018). Furthermore, the carbon quantum dots have shown improved surface-to-volume ratios, well-defined stoichiometry, and crystallinity (Arumugham et al., 2022; Gong et al., 2022; Rusmin et al., 2022). Among the most promising photocatalysts are carbon quantum dots, which are characterized by zero photo-attrition, facile electron transmission, excellent stability, and excellent photocatalytic activity. Quantum dots made of carbon are chemically inert, thermally stable, eco-friendly, and environmentally friendly. In recent years, several methods have been proposed to synthesize carbon materials, especially

carbon quantum dots, and their effectiveness in photocatalytic applications has been demonstrated (Rajabi et al., 2016). Laser ablation (Huang et al., 2022), hydrothermal oxidation (Sabet and Mahdavi, 2019; Huang et al., 2022) and pyrolysis (Zhu et al., 2022) are some examples of these synthetic methods. There are certain issues and challenges associated with some synthesis techniques, such as complicated instrumental configurations, uncontrolled chemical reaction conditions, poor spectral performance, and limited yields. Nonetheless, in recent years, green mediated synthesis of carbon materials, particularly carbon quantum dots, has been increasingly popular among researchers (Gu et al., 2020; Hui et al., 2021; Nugraha et al., 2021). In the green synthesis of luminescent carbon, low temperature aqueous growth methods followed by pyrolysis are rarely used. Aqueous methods use a low temperature to activate the functional groups and enhance the surface active sites, while mild pyrolysis removes excess groups from the carbon surface, resulting in modified surfaces based luminescent carbon archives. Specifically, a low temperature aqueous treatment followed by the mild pyrolysis of *Citrullus Colocynthis* are combined to produce photocatalytic carbon material (Arízaga et al., 2022).

By using this method, it is possible to achieve high efficiency photocatalytic oxidation of methylene blue in aqueous solution. *Citrullus Colocynthis* is a desert plant that grows on sandy and arid soils. It is abundant, contains high levels of natural products, and is widely distributed, making it an excellent source for the synthesis of carbon materials for applications such as photocatalytic adsorption and oxidation of organic dyes.

Aqueous chemical growth followed by mild pyrolysis was used in this study to prepare a photocatalytic carbon material made from *Citrullus Colocynthis*. The carbon material was subjected to several spectroscopic measurements, including scanning electron microscopy (SEM), X-ray diffraction (XRD), Fourier transform infrared spectroscopy (FTIR), Dynamic light scattering (DLS), and UV-visible spectrophotometry. The as-prepared carbon material was evaluated for its ability to catalyze the oxidation of MB in aqueous solutions, and it was found that, at low concentrations, almost 100% of the dye was removed.

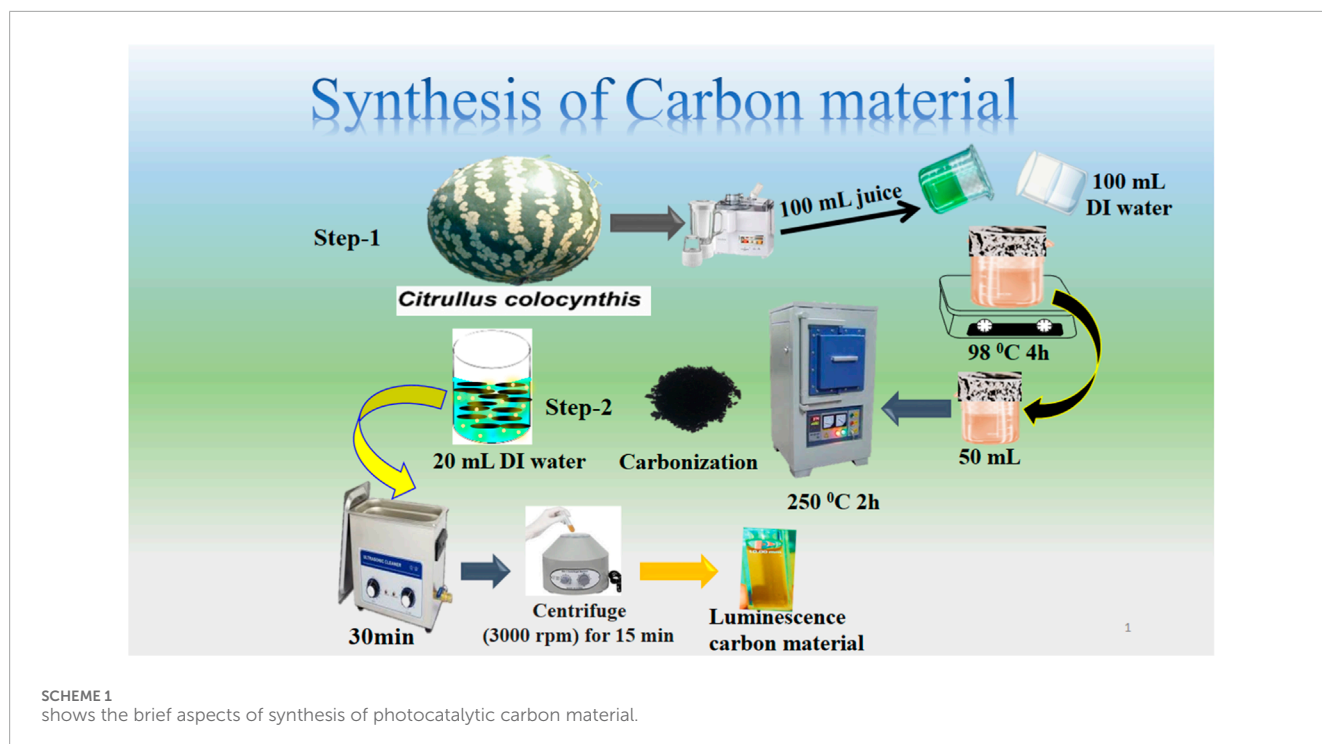
## 2 Materials and methods

### 2.1 Chemical and reagents

Sigma Aldrich and Merck, Karachi Sindh, Pakistan, provided methylene blue (C<sub>16</sub>H<sub>18</sub>ClN<sub>3</sub>S, Mm 319.85 g/mol), sodium hydroxide (NaOH, Mm 39.997 g/mol), hydrochloric acid (HCl), ascorbic acid (C<sub>6</sub>H<sub>8</sub>O<sub>6</sub>) and sodium borohydride (NaBH<sub>4</sub>). Throughout the experiment, high analytical grade chemicals and ultrapure water were used.

### 2.2 Synthesis of carbon material from *Citrullus colocynthis*

As described in Scheme 1, carbon material was synthesized by using an aqueous chemical growth method at low temperatures followed by mild pyrolysis. To begin with, *Citrullus Colocynthis* was collected during the summer season from a deserted area



in district Qamabar Shahdad Kot Sindh, Pakistan. Afterwards, *Citrullus Colocynthis* was sliced and juiced using a juicer machine. Following that, 100 mL of *Citrullus Colocynthis* juice was mixed with 100 mL of deionized water, covered with aluminum sheet and boiled at 98 °C for 4 hours. It was necessary to treat the mixture at low temperatures in order to obtain a desired amount of carbon with a favorable active surface for the application of photocatalysis. In the second step, 50 mL of the boiled mixture was placed into Pyrex glass of 100 mL and kept in a muffle furnace at 250°C for 2 h at a ramp rate of 15°C per minute. After sonicating for 50 min, the solution was centrifuged at 5,000 rotations per minute for 30 min to remove the larger carbon particles. We were able to recover 0.4 g of dark brown carbon for further characterization and analysis. The carbon yield percentage based on the use of 50 mL of the boiled mixture and recovery of 0.4 g of carbon were estimated about 0.8%. The following is a brief description of the steps involved in producing photocatalytic carbon material (Scheme 1).

### 2.3 Characterizations of prepared carbon material

Using X-ray diffraction (XRD), the crystal structure of as prepared carbon was analyzed (Cu K $\alpha$  radiation with a wavelength of 0.15406 nm at a scanning range of 10–80, Bruker D8 advance). The morphology of carbon material prepared from *Citrullus Colocynthis* was examined using a scanning electron microscope (Hitachi Regulus 8,100, Tokyo, Japan), and the functional groups were identified using an FT-IR spectrometer (Tensor 27, Bruker Optics, Ettlingen, Germany). Carbon and dye degradation were assessed using UV-visible spectroscopy (Lambda 365, PerkinElmer, Waltham, MA, United States) in the wavelength range of 200–800 nm.

### 2.4 Photodegradation of methylene blue using as prepared carbon material

As obtained, carbon material from *Citrullus Colocynthis* was evaluated under UV light irradiation for its photocatalytic activity using UV-visible absorbance spectrometry. In a quartz jar containing 250 mL of deionized water, different concentrations of MB were prepared, including  $2.3 \times 10^{-5}$  M,  $1.5 \times 10^{-5}$  M and  $0.6 \times 10^{-5}$  M. The MB solutions were consistently mixed with 5 mg of carbon material until the dye was absorbed and fully mixed into the carbon surface. A well-established equilibrium between adsorption and desorption was observed after constant stirring for 30 min. Following irradiation of dye solutions with UV light, every 15 min interval was recorded for the decrease in absorbance. A spectrophotometer associated with a 300 W Xenon lamp with a wavelength range of 200–800 nm was used to detect the decrease in UV-visible absorbance. The homemade UV box was built using six light emitting diodes having a wavelength of 365 nm and power of 12 W. In controlled conditions, the dye removal was monitored by observing the decrease in color intensity, the decrease in UV light absorbance, and the time factor. Throughout the irradiation of ultraviolet light, the reaction jar was constantly stirred. All sources of light were cut off during the photodegradation of MB, and the reaction jar was primarily irradiated with UV light in the UV box. Following is a formula for estimating the removal percentage of MB:

$$\%D = \frac{A_0 - A_t}{A_0} \times 100\% \quad (1)$$

Herein,  $A_0$  and  $A_t$  are initial and after degradation concentrations of MB, while the %D indicate the degradation percentage of MB.

## 3 Results and discussion

### 3.1 Structural studies of carbon material synthesized from *Citrullus colocynthis*

A scanning electron microscope was used to examine the shape of carbon as prepared using *Citrullus Colocynthis*, and the SEM images at two varying resolutions are shown in Figures 1A,B. According to the obtained morphological information, the carbon material exhibits an irregular graphitic sheet like shape. As illustrated in Figures 1A,B, sheets may have a thickness of a few microns. The functional groups information of as prepared carbon material was obtained from FTIR analysis as shown in Figure 1C. In Figure 1C, we can see that the stretching vibration frequency of 3,432  $\text{cm}^{-1}$  was attributed to the hydroxyl groups (O-H) attached to the surface of the carbon material, while the C-H stretching band was positioned at 2,926  $\text{cm}^{-1}$ . The band at 2,509  $\text{cm}^{-1}$  has been attributed to SH and the stretching band at 1808  $\text{cm}^{-1}$  has been attributed to the stretching vibration band of C=O bonds. C-O and N-H are indexed to the stretching and bending vibrations at 1,578  $\text{cm}^{-1}$  (Yanget al., 2012), while the stretching bands for C-N, N-H, and -COOH are observed at 1,424  $\text{cm}^{-1}$ . As a result of the FTIR study, several reducing groups such as -OH, -NH<sub>2</sub>, and -COO were observed to be adsorbing on the surface of the carbon material. These findings are in agreement with previous studies (Tetsuka et al., 2012; Jin et al., 2013; Sugiarti and Dharmawan, 2015; Zhang et al., 2015). Figure 1D illustrates the spectrum generated by UV-visible spectroscopy in aqueous solution when the optical properties of the carbon material were studied. The shoulder peak at 344 nm in the absorbance spectrum has described the  $n-\pi^*$  transition of CO and found in good agreement with the published work (Rezaei et al., 2019). It is possible to assign the absorbance peaks at 318 nm, 323 nm, and 333 nm to an sp<sup>2</sup> hybrid configuration of aromatic carbon, which is a typical characteristic of graphite like carbon materials (Eda et al., 2009). As indicated by the UV-visible spectrum, the graphite of the as-prepared carbon material has typical characteristics, as verified by the published results (Pan et al., 2010; Zheng et al., 2013). As synthesized carbon material was examined by XRD for its crystalline properties, and the measured diffraction patterns are shown in Figure 2. In XRD analysis, reflections were observed at 19.59° and 44.53°, respectively, and corresponded to crystal planes (001) and (101). Based on the XRD analysis, it has been confirmed that the (101) reflection peak is highly intense, which indicates that the material prepared exhibits weak crystalline characteristics. Figure 2A is accompanied by an inset explaining the behavior of synthetic carbon material made from *Citrullus Colocynthis* with illuminated UV light. During the day, the carbon material emits a light brown color, while when exposed to UV light, it emits a blue color, indicating zero hazards and high environmental friendliness for use in photocatalytic applications. Furthermore, the bandgap transitions, which were shown to correlate with the surface defects present in the CQDs, were mainly responsible for the luminescent features. The effect of the fluorescence features of the CQDs may also be responsible for the modest variations in particle size distribution and the sp<sup>2</sup> hybridization of carbon clusters. Moreover, the greater excitation intensity of the CQDs resulted in larger energy emissions by the material, influencing its luminescent characteristics (Nizam, et al., 2023). Carbon material

prepared in this manner is hydrophilic, which makes it a potential candidate for the photodegradation of MB. In the inset image, the carbon material was dispersed in water, then 1 mL of it was placed in quartz glass cuvette and irradiated with ultraviolet light for 3 minutes. A mobile camera was used to collect the image. Figure 2B provides information on the particle size of the carbon material as obtained using a Zeta sizer. Based on the SEM analysis, the size of the carbon material was observed in the micro dimension. The optical properties of carbon material materials have been found useful for photocatalytic applications (Yang et al., 2017; Cong et al., 2023). For this reason, we have performed the UV-visible absorption measurement and the presence of edges was noticed between 390–450 nm as shown in Figure 3A. The Kubelka-Munk model was used to estimate the optical band gap via extrapolation plot of  $(ah\nu)^2$  vs.  $h\nu$ , as shown in Figure 3B. Whereas, the  $h\nu$  as energy of photons, both  $n$  and  $A$  known as constants, E.g., corresponded to band gap energy and  $\alpha$  as absorption coefficient. The optical band gap value of as synthesized carbon material was found about 2.52 eV. The optical band gap analysis has indicated the semiconducting nature of as synthesized carbon material.

### 3.2 Photodegradation of MB in aqueous solution using as prepared carbon material from *Citrullus colocynthis*

Supplementary Figure S1 depicts the breakdown of MB dye at  $2.3 \times 10^{-5}$  M using UV light, without the use of manufactured carbon material from *Citrullus Colocynthis* extract. Supplementary Figure S1A shows a restricted kinetic response with minor absorbance variations, demonstrating that UV radiation has a negligible impact on the breakdown process of MB. The kinetic parameters were also studied to illustrate the reaction process, as illustrated in Supplementary Figure S1B,C. These results show that the rate constant value was very low, and UV radiation had a minor effect on the degradation process. The deterioration efficiency of MB utilizing simply UV light exposure was found to be around 12%, defining the low performance of MB oxidation as illustrated in Supplementary Figure S1D. At fixed intervals of 15 min, 10 min and 5 min, Figures 4–6 illustrates the degradation profile for three different concentrations of MB,  $2.3 \times 10^{-5}$  M,  $1.5 \times 10^{-5}$  M and  $0.6 \times 10^{-5}$  M, respectively, resulting in a decrease in UV-visible absorbance spectra and percent (%) dye removal. Based on the results of this study, we found that dye concentration plays an important role in the evaluation of the performance of the proposed carbon material. Figure 6 shows that a lower MB concentration significantly reduced the UV-visible absorbance of the carbon material. Similarly, the % removal of MB was highly increased when MB  $0.6 \times 10^{-5}$  M concentration was utilized, which suggests that the carbon material as prepared has a dye removal capacity of almost 99.8%. Figures 4, 5 indicate that the dye removal efficiency for MB concentrations of  $2.3 \times 10^{-5}$  M and  $1.5 \times 10^{-5}$  M is close to 97.1% and 97.9%, respectively. Furthermore, the reaction kinetics of MB onto the surface of as synthesized carbon material was determined using a pseudo-first order kinetic equation that included irradiation time intervals (min) and  $k$  as a first order velocity constant. The value of  $k$  measures the photocatalytic activity, with a higher value of  $k$  indicating increased photocatalytic

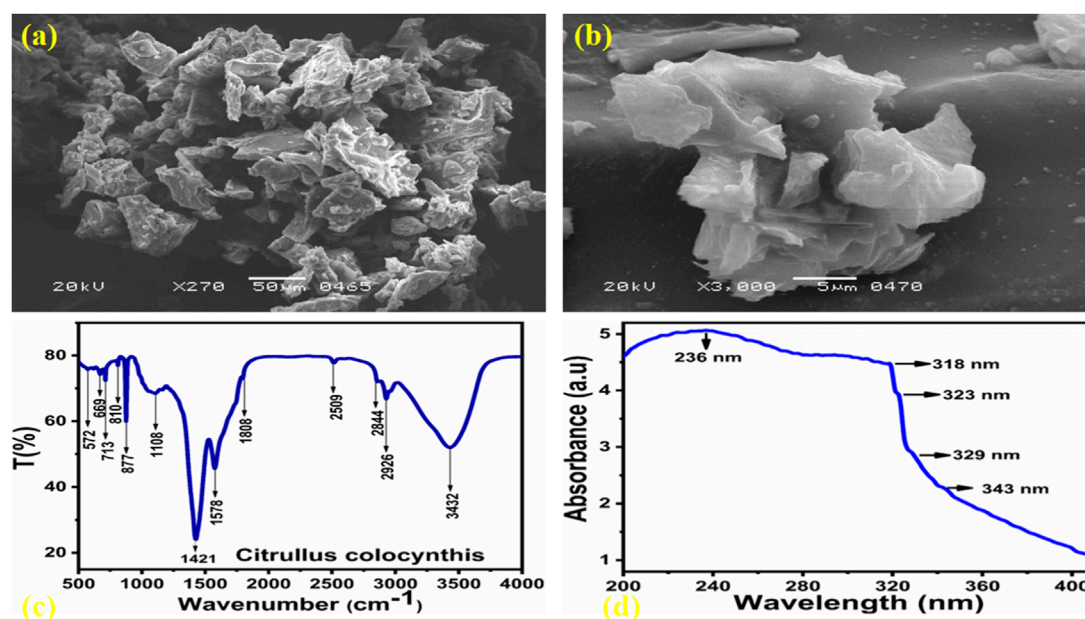


FIGURE 1 (A and B) SEM images of carbon material prepared from *Citrullus Colocynthis* at different magnifications, (C) FTIR spectrum for functional group analysis, (D) UV-visible absorbance spectrum of carbon material prepared from *Citrullus Colocynthis*.

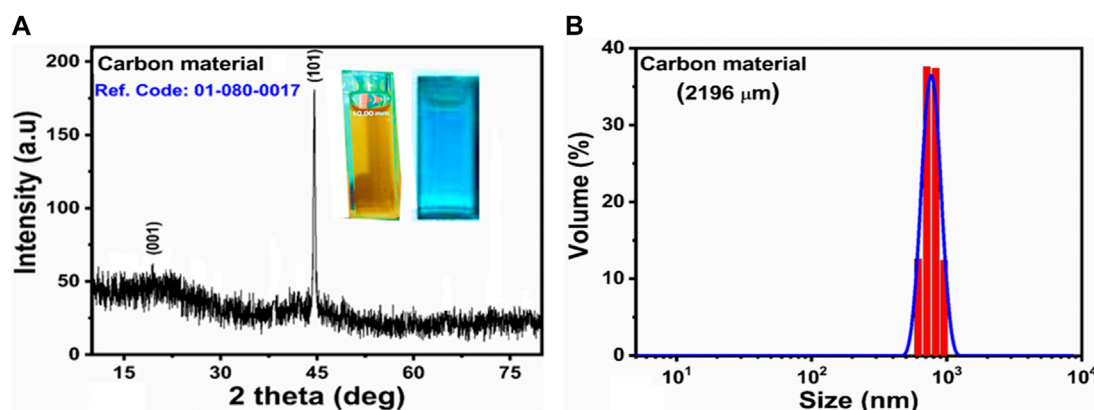


FIGURE 2 (A) XRD diffraction reflections of carbon material, the inset describes the luminescent properties carbon material, (B) DLS analysis of as synthesized carbon material.

efficiency (Katheresan et al., 2018; Panagopoulos, 2022a). Based on the results presented in Figure 4A–C, Figure 5A–C, Figure 6A–C with their linear fitted lines, Figure 7 shows the relationship between concentration and irradiation time. As a result of a linear fit, the value of slope corresponding to the first order reaction was used to estimate the rate constant. From the kinetics study, it was observed that the degradation rate was higher in the lowest dye concentration compared to the highest dye concentration. However, the reaction rate at higher MB concentrations was decreased due to the significant barriers provided by the large adsorbed dye molecules on the surface of carbon material for UV photons to react. This resulted in the highest removal % of MB at the lowest concentration of MB.

In addition, pH has been found to play an essential role in evaluating the photocatalytic performance of photocatalysts due to the accumulation of charges on the surface of the catalysts and the depth of activation towards specific pollutants (Yang et al., 2021). As shown in Supplementary Figure S1, the carbon material was used in order to understand the role of pH at pH values ranging from 5 to 11 in  $0.6 \times 10^{-5}$  M MB. In comparison to pH 7, nine and 11, there is a considerable decrease in the absorbance at pH 5, indicating that the surface of the synthesized carbon material is highly functional and activated. There is also a significant effect of pH variation on the dye removal percentage in dye solutions. A pH adjustment of 2M HCl and 2M NaOH was used to study the pH effect in the  $2.3 \times 10^{-5}$  M MB. With no acid or base present, the pH of dye solution was

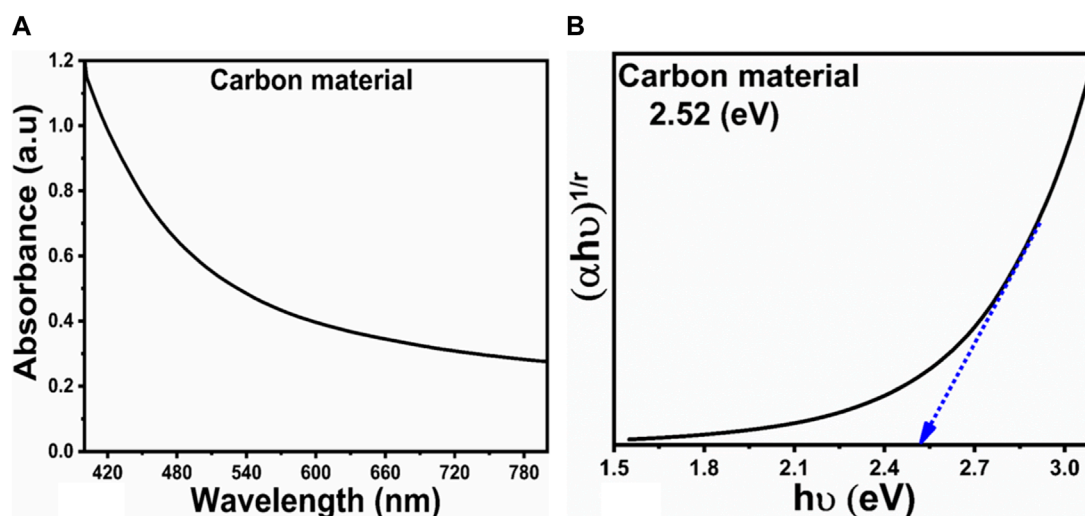


FIGURE 3 (A) Optical absorbance of as synthesized carbon material (B) Kubelka-Munk plot synthesized carbon material.

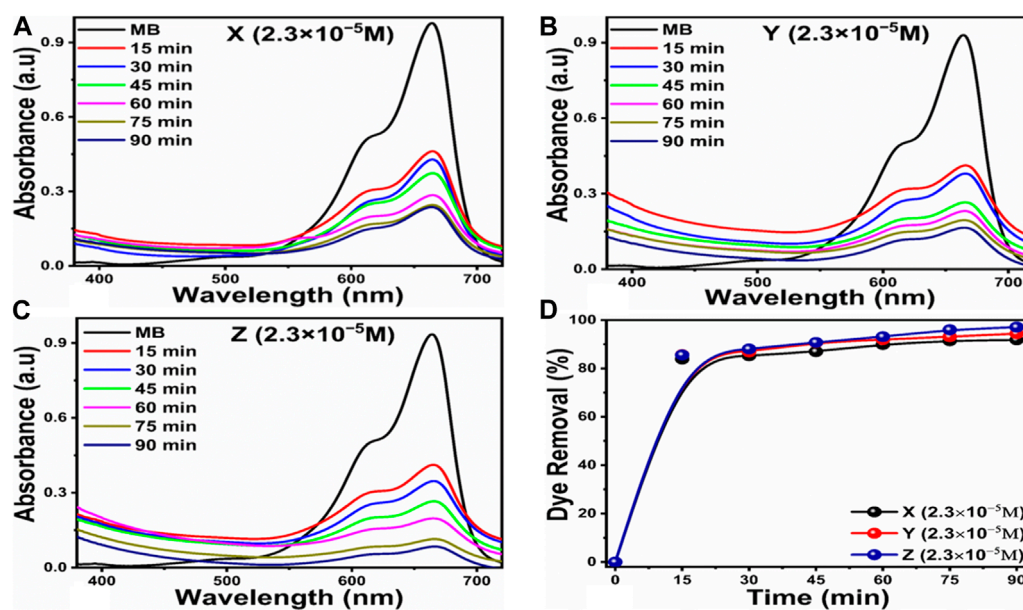


FIGURE 4 UV-visible absorbance spectra for the degradation of MB with initial concentration of  $2.3 \times 10^{-5}$  M for the time period of 90 min under the illumination of UV light (A) photocatalyst dose of 5 mg, (B) photocatalyst dose of 10 mg, (C) photocatalyst dose of 15 mg, (D) Corresponding degradation efficiency of MB.

approximately 6.5. Lower and higher pH values were adjusted using 2M HCl and NaOH solutions, respectively. In comparison with other pH values of dye solution, the degradation of MB was dominated by the acidic pH of 5. As a result of the catalyst generating more holes, it can effectively participate in the degradation of MB. In contrast, at pH 11, dye molecules are largely adsorption on the surface of carbon material, providing less surface area for interactions with UV photons and hydroxyl radical generation, thus reducing the oxidation rate of dye (Marszewski et al., 2016). A kinetic analysis of the reaction rate was also conducted using Eq. (1); this analysis is

shown in Figures 7A,B. It was found that the reaction rate constant of MB degradation was higher at pH five than at other pH values of MB solution under the influence of different pH values. According to Figure 7C, the dye removal % was almost 100% according to an estimate of degradation efficiency. The different pH values of the MB solution indicate that pH plays a significant role in the removal of dye from aqueous solutions, and the proposed carbon material has the potential to nearly remove MB at pH 5. The pH of dye solution may change the point of charge on the surface of photocatalyst and favoring the degradation of MB, hence it might

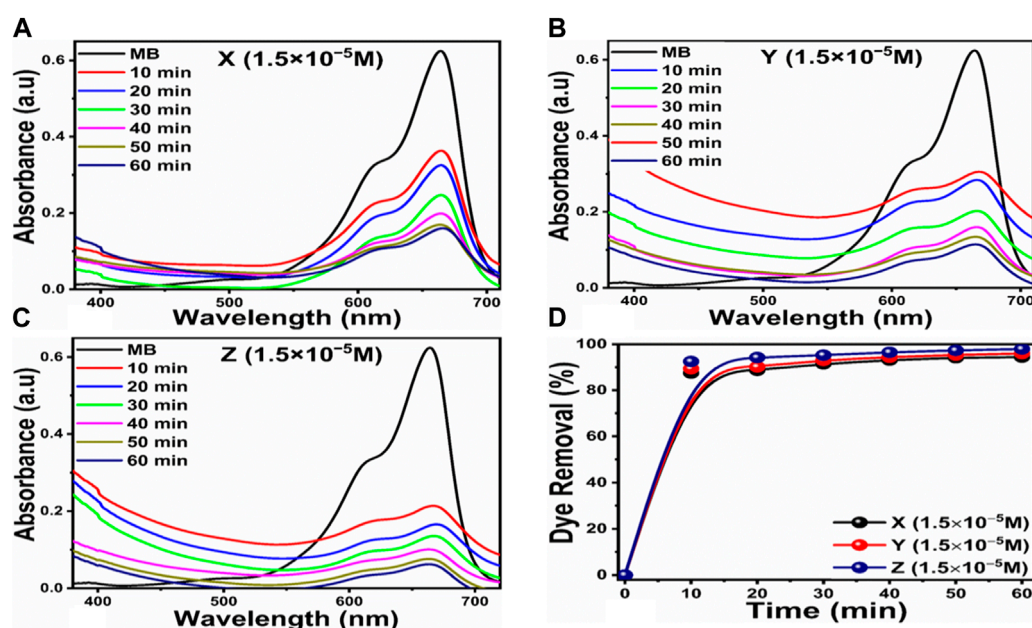


FIGURE 5 UV-visible absorbance spectra for the degradation of MB with initial concentration of  $1.5 \times 10^{-5}$  M for the time period of 60 min under the illumination of UV light (A) photocatalyst dose of 5 mg, (B) photocatalyst dose of 10 mg, (C) photocatalyst dose of 15 mg, (D) Corresponding degradation efficiency of MB.

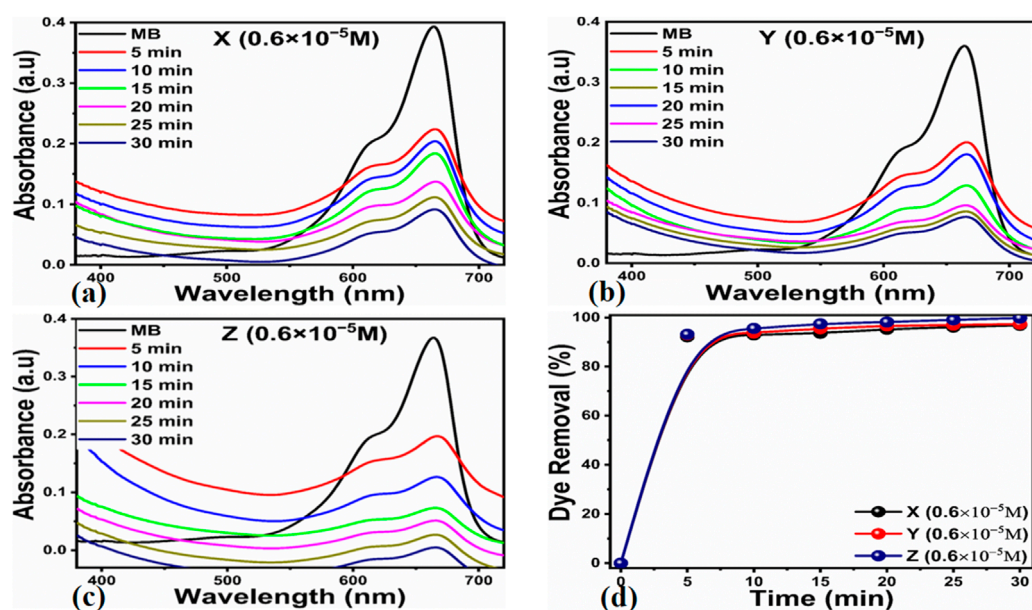
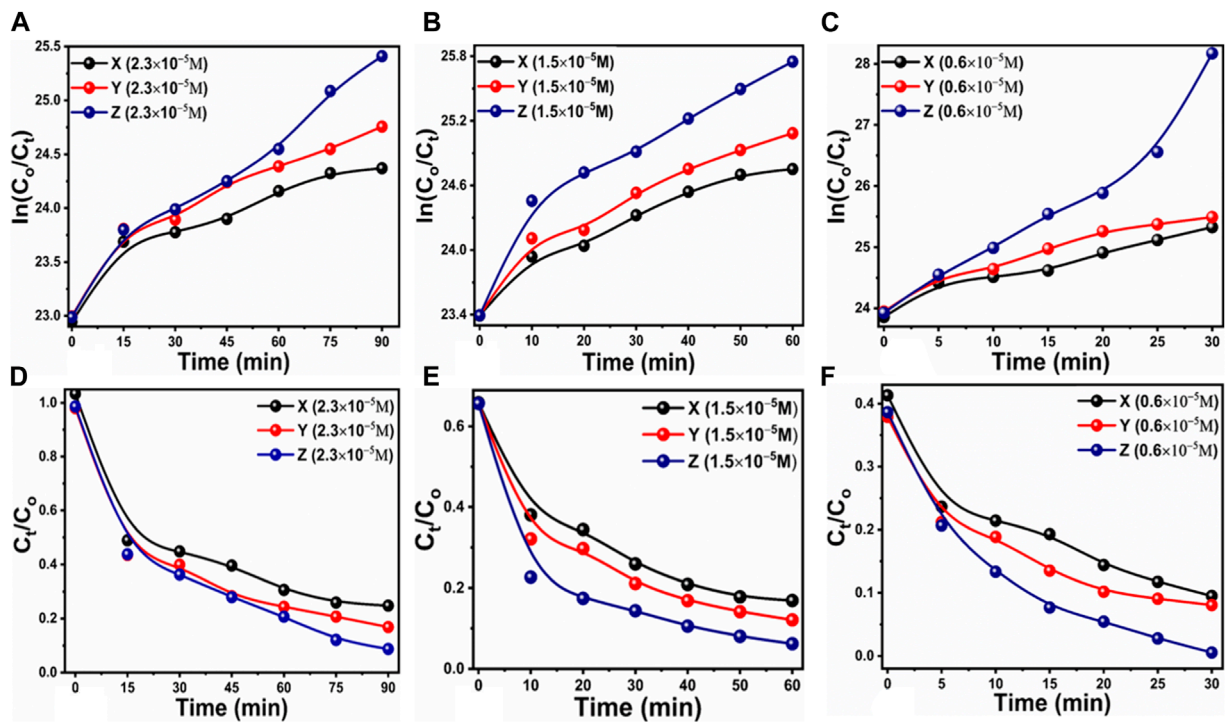


FIGURE 6 UV-visible absorbance spectra for the degradation of MB with initial concentration of  $0.6 \times 10^{-5}$  M for the time period of 30 min under the illumination of UV light (A) photocatalyst dose of 5 mg, (B) photocatalyst dose of 10 mg, (C) photocatalyst dose of 15 mg, (D) Corresponding degradation efficiency of MB.

play a role for the efficient of degradation of MB at pH 5. It is essential to understand the role of radicals in the degradation of MB in order to propose a mechanism for its degradation. To accomplish this, we conducted a scavenger test using ascorbic acid, ethylene-ediamine tetramine (EDTA) and sodium borohydride in an environment of

$2.3 \times 10^{-5}$  MB, and Figure 8D illustrates the degradation of carbon material in this environment. Previously, it has been shown that the hydroxyl ( $\cdot\text{OH}$ ), photogenerated holes ( $h^+$ ) and superoxide radical ions ( $\cdot\text{O}_2^-$ ) radicals have been responsible for the degradation of dyes. In this study, the selected scavengers generated hydroxyl and



**FIGURE 7** Degradation kinetics (A) linear plot of the natural logarithm of dye concentration of  $C_0$  initial and  $C_t$  after certain intervals of time at an MB concentration of  $2.3 \times 10^{-5}$  M using different catalyst doses of 5, 10, and 15 mg for the time period of 140 min, (B) linear plot of same catalyst doses but in low concentration of  $1.5 \times 10^{-5}$  M 60 min, (C) linear plot of same catalyst doses in dye concentration of  $0.6 \times 10^{-5}$  M 30 min, (D) linear plot of MB concentration of  $2.3 \times 10^{-5}$  M with different catalysts doses of 5, 10, and 15 mg for 90 min, (E) linear plot of MB concentration of  $1.5 \times 10^{-5}$  M with different catalysts doses of 5, 10, and 15 mg for 60 min (F) linear plot of MB concentration of  $0.5 \times 10^{-5}$  M with different catalysts doses of 5, 10, and 15 mg for 30 min.

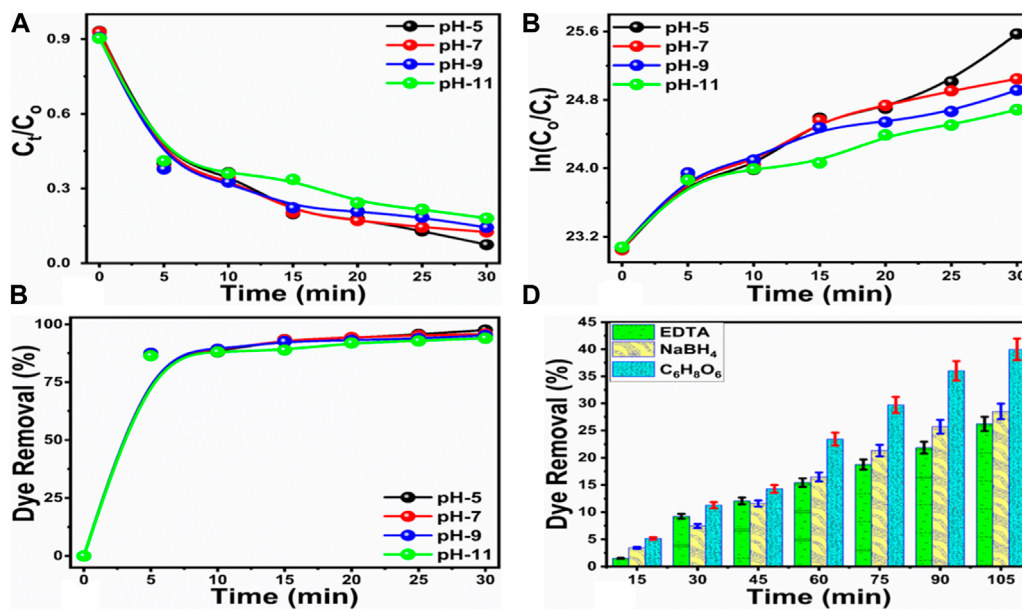


**FIGURE 8** (A) Linear plot of the natural logarithm of dye concentration  $2.3 \times 10^{-5}$  M using 15 mg during 30 min at pH values 5, 7, 9, and 11, (B) linear plot of dye concentration  $2.3 \times 10^{-5}$  M using catalyst dose 15 mg during 30 min at pH values 5, 7, 9, and 11, (C) degradation efficiency during dye  $2.3 \times 10^{-5}$  M and catalyst dose of 15 mg at pH values of 5, 7, 9, and 11 for the time period of 30 min, (D) (C) degradation inhibition efficiency in the presence of various scavengers using  $2.3 \times 10^{-5}$  M MB and catalyst dose of 15 mg with the illumination of UV light.

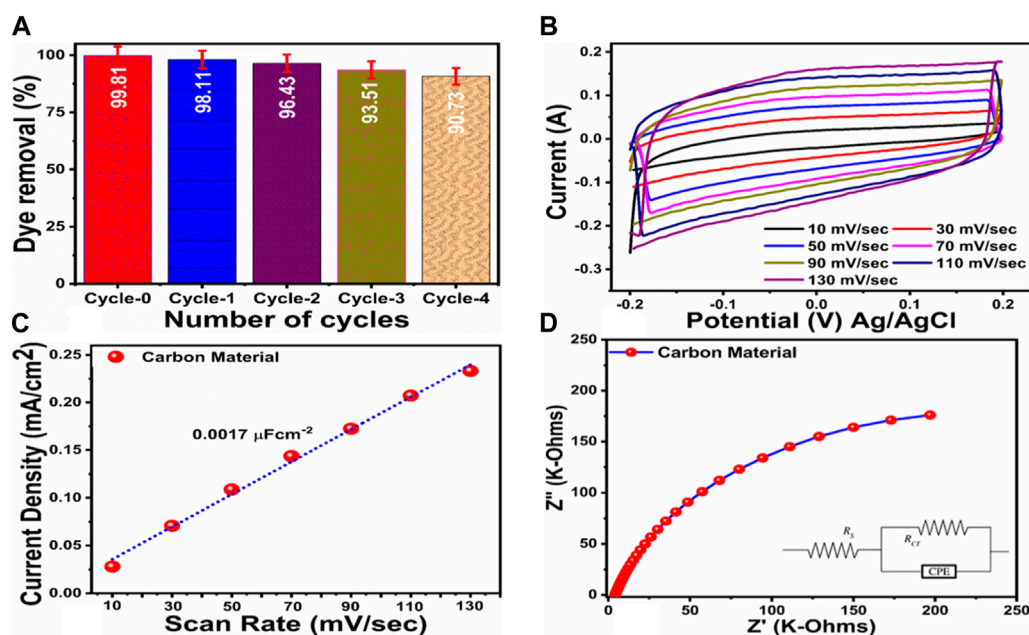
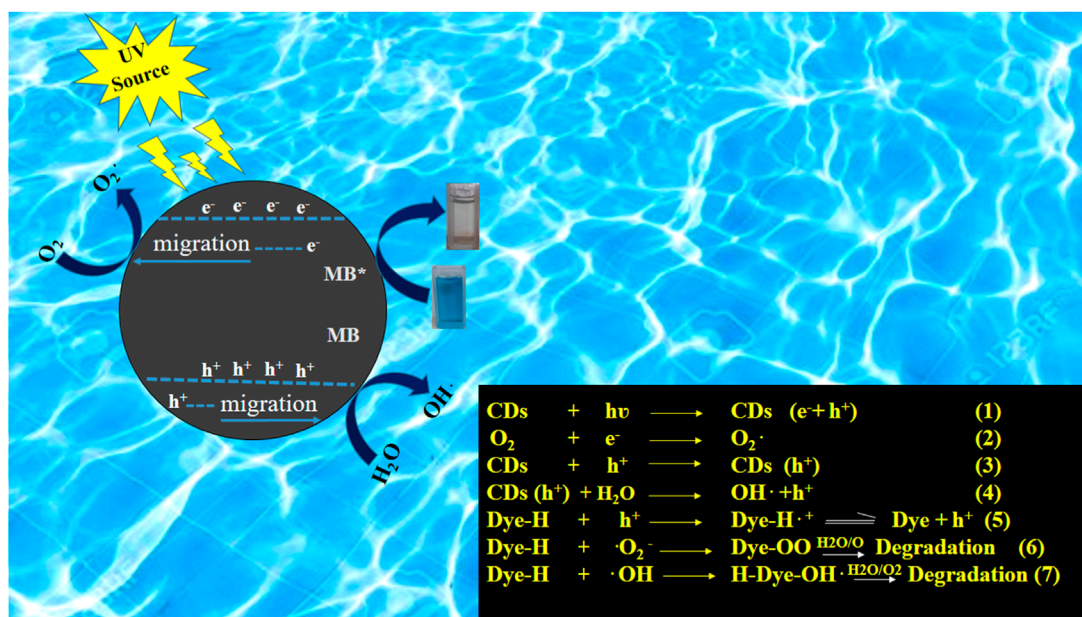


**FIGURE 9** (A) % photodegradation efficiency of MB during recycling stability using concentration of  $2.3 \times 10^{-5}$  M and 15 mg catalyst dose (B) Cyclic voltammety polarization curves at different sweeping scan rates using concentration of  $2.3 \times 10^{-5}$  M of MB, (C) Corresponding linear plot for the estimation of ECSA, (D) EIS spectrum of carbon material using MB concentration  $2.3 \times 10^{-5}$  M, inset is showing the fitted equivalent circuit.



oxygen radicals (Shelar et al., 2020). These radicals were primarily responsible for the degradation of MB in the laboratory (Molla et al., 2017; Mondol et al., 2021). In the scavenger analysis, it was found that EDTA significantly decreased the degradation of MB, indicating that the hydroxyl radicals (OH) are mainly responsible for the degradation of MB when using the prepared carbon material in

Figure 7D. The reusability test was also conducted to confirm the long-term durability of the carbon material and five reusable dye degradation tests of  $2.3 \times 10^{-5}$  M MB were conducted as shown in Figure 9A. The results of one controlled test and four reusable tests are presented in Figure 8A under UV irradiation. Following the proper washing and storage of the synthesized carbon material,

it was evident that it could be used for several measurements with nearly the same degradation efficiency. According to Figure 8A, the degradation efficiency for cycle 0, cycle 1, cycle 2, cycle 3, and cycle four was 99.81%, 98.11%, 96.43%, 93.51%, and 90.73%, respectively. Even after four reusable tests, the degradation efficiency did not significantly decrease, indicating that the proposed carbon material could serve as an effective photocatalyst for wastewater treatment. Furthermore for the description of point of difference between the photocatalytic and adsorption properties of as synthesized carbon, the adsorption experiment was conducted but the results of dye removal percentage were noticed very poor. Whereas using photocatalytic approach the removal percentage of MB was highly efficient, supported the aims of proposed study about the design of photocatalytic carbon materials using green synthesis. Hence, the dye removal performance of as prepared carbon material based on the photocatalytic oxidation are reported in this study. The rapid and high efficiency of photocatalytic method have been seen in the literature, therefore the design of low cost, efficient, simple, scale up and environment friendly photocatalysts are highly desirable. According to Figure 7B, electrochemical active surface area was estimated using cyclic voltammetry with non-faradic region at different scan rates to demonstrate improved performance of the synthesized carbon material towards degradation of MB under UV illumination. The calculation of electrochemical active surface area (ECSA) was done using reported work (Laghari et al., 2023). An analysis of the linear plot of the difference between the current density on the anodic and cathodic sides against various scan rates has yielded a value of ECSA around  $0.0017 \mu \text{ cm}^{-2}$  as shown in Figure 8C. According to the estimated value of ECSA, the carbon material displayed a significant amount of surface active sites which could play a vital role in the degradation of MB under UV light irradiation. As shown in Figure 8D, electrochemical impedance spectroscopy (EIS) was used to evaluate the charge transfer rate in order to enhance the degradation performance of the carbon material. Z-view software was used to fit the raw data of EIS, and the equivalent circuit is shown in the inset of Figure 9D. According to the equivalent circuit, there was a constant phase element (CPE), a solution resistance ( $R_s$ ), and a charge transfer resistance ( $R_{ct}$ ). There is good agreement between the results presented in the EIS and those published in the literature (Hartanto et al., 2022). The small semicircle of the Nyquist plot indicates that the carbon material exhibited good conductivity and a high charge transfer rate. ECSA and EIS results reveal that the enriched active surface area and rapid charge transfer rate influenced the degradation of MB under the illumination of UV light. Hence, CV and EIS were used to illustrate the exposed active surface area and charge transfer rate for dynamic degradation of dye. Because the exposure of active surface area and the charge transfer could provide two aspects, active surface area for high interaction of dye molecules and charge transfer for causing the creation of more radicals during the interaction with water, hence rapid dye degradation could be expected. Scheme 2 describes the degradation mechanism of MB on photocatalytic carbon material can be described generally as follows. As a result of the UV light interaction with the carbon material, electron and hole pairs are transferred from the valence band to the conduction band. The electrons and holes then interact with the water molecules, generating radicals like superoxide and hydroxyl that contribute to dye degradation. MB dye

is then converted into harmless products. Supplementary Table S1 summarizes the performance of photocatalytic carbon towards MB degradation, whereas Supplementary Table S2 compares the photocatalytic activity of carbon material with those of several recently reported catalysts. In comparison with previously reported catalysts, the proposed carbon material is facile, low cost, highly efficient, and environmentally friendly, which makes it potentially useful for wastewater treatment.

## 4 Conclusion

By using a low temperature aqueous chemical growth method combined with mild pyrolysis, we were able to prepare a low cost and earth abundant microstructure carbon material from *Citrullus Colocynthis*. An analysis of morphology, crystalline quality, optical properties, and particle size was carried out using SEM, XRD, UV-visible, and DLS techniques. Due to its luminescent properties and abundant surface active sites, the carbon material showed efficient photodegradation of MB in aqueous solution. MB was degraded under the influence of UV light and various parameters were examined, including the concentration of the initial dye, the pH of the dye solution, the scavenger and the recycling process. The carbon material performed better at pH five than at other pH values of dye solutions. As prepared carbon material exhibited excellent recycle stability, indicating its potential for long-term use as a water treatment material. Based on the results of ECSA and EIS, the performance of as prepared carbon material was highly enhanced due to the presence of abundant surface active sites and the rapid rate of charge transfer. Since *Citrullus Colocynthis* is a deserted plant, widely distributed across many regions, and eco-friendly, it can provide a roadmap for development of facile and inexpensive high-performance photocatalysts.

## Data availability statement

The raw data supporting the conclusion of this article will be made available by the authors, without undue reservation.

## Author contributions

MB: Data curation, Investigation, Writing—original draft, Writing—review and editing. ED: Formal Analysis, Methodology, Visualization, Writing—review and editing, Writing—original draft. AT: Formal Analysis, Methodology, Writing—review and editing, Writing—original draft. AH: Data curation, Investigation, Writing—review and editing, Writing—original draft. IH: Methodology, Resources, Writing—review and editing, Writing—original draft. SC: Investigation, Methodology, Writing—review and editing, Writing—original draft. AS: Data curation, Formal Analysis, Investigation, Writing—review and editing, Writing—original draft. AN: Validation, Writing—review and editing, Writing—original draft. MT: Formal Analysis, Visualization, Writing—review and editing, Writing—original draft. AH: Formal Analysis, Investigation, Writing—review and

editing, Writing—original draft. ZI: Conceptualization, Supervision, Writing—original draft, Writing—review and editing.

## Funding

The author(s) declare that no financial support was received for the research, authorship, and/or publication of this article.

## Acknowledgments

The authors would like to gratefully acknowledge the Higher Education Commission Pakistan for partial support under the project NRPU/8350/8330. We also extend our sincere appreciation to the Researchers Supporting Project Number (RSP 2024R79) at King Saud University, Riyadh, Saudi Arabia. The authors would like to acknowledge the partial support of Ajman University, Internal Research Grant Nos. DRGS ref. 2023-IRG-HBS-2, RTG-2023-HBS-01.

## References

- Arizaga, G. G. C., Galván, J. G. Q., Bail, A., González, A. L. P., Nuñez, C. P., and Álvarez, M. Á. L. (2022). Green approach to synthesize functional carbon nanoparticles at low temperature. *Sustain. Chem. Clim. Action* 1, 100002. doi:10.1016/j.scca.2022.100002
- Arumugham, N., Mariappan, A., Eswaran, J., Daniel, S., Kanthapazham, R., and Kathirvel, P. (2022). Nickel ferrite-based composites and its photocatalytic application—A review. *J. Hazard. Mater. Adv.* 8, 100156. doi:10.1016/j.hazadv.2022.100156
- Chen, X., Lai, D., Yuan, B., and Fu, M. L. (2020). Fabrication of superelastic and highly conductive graphene aerogels by precisely “unlocking” the oxygenated groups on graphene oxide sheets. *Carbon* 162, 552–561. doi:10.1016/j.carbon.2020.02.082
- Cong, C. Q., Dat, N. M., Hai, N. D., Nam, N. T. H., An, H., Do Dat, T., et al. (2023). Green synthesis of carbon-doped zinc oxide using *Garcinia mangostana* peel extract: characterization, photocatalytic degradation, and hydrogen peroxide production. *J. Clean. Prod.* 392, 136269. doi:10.1016/j.jclepro.2023.136269
- Cong, S., and Zhao, Z. (2018). Carbon Quantum Dots: a component of efficient visible light photocatalysts. *Visible-Light Photocatal. Carbon-Based Materials*. Eda. doi:10.5772/intechopen.70801
- Eda, G., Lin, Y. Y., Mattevi, C., Yamaguchi, H., Chen, H. A., Chen, I. S. C. W., et al. (2009). Blue photoluminescence from chemically derived graphene oxide. *arXiv Prepr. arXiv:0909.2456*. doi:10.48550/arXiv.0909.2456
- Feng, S., Chen, T., Liu, Z., Shi, J., Yue, X., and Li, Y. (2020). Z-scheme CdS/CQDs/g-C<sub>3</sub>N<sub>4</sub> composites with visible-near-infrared light response for efficient photocatalytic organic pollutant degradation. *Sci. total Environ.* 704, 135404. doi:10.1016/j.scitotenv.2019.135404
- Ghosh, U., and Pal, A. (2020). Fabrication of a novel Bi<sub>2</sub>O<sub>3</sub> nanoparticle impregnated nitrogen vacant 2D g-C<sub>3</sub>N<sub>4</sub> nanosheet Z scheme photocatalyst for improved degradation of methylene blue dye under LED light illumination. *Appl. Surf. Sci.* 507, 144965. doi:10.1016/j.apsusc.2019.144965
- Gong, D., Li, X., Zhang, X., Zhang, W., Chen, T., and Zhang, X. (2022). Green fabrication of functionalized graphene quantum dots prepared from photocatalytic activity for the degradation of new cocaine. *Food Chem.* 387, 132928. doi:10.1016/j.foodchem.2022.132928
- Gu, S., Hsieh, C. T., Yuan, C. Y., Gandomi, Y. A., Chang, J. K., Fu, C. C., et al. (2020). Fluorescence of functionalized graphene quantum dots prepared from infrared-assisted pyrolysis of citric acid and urea. *J. Luminescence* 217, 116774. doi:10.1016/j.jlumin.2019.116774
- Gupta, B. K., Kedawat, G., Agrawal, Y., Kumar, P., Dwivedi, J., and Dhawan, S. K. (2015). A novel strategy to enhance ultraviolet light driven photocatalysis from graphene quantum dots infilled TiO<sub>2</sub> nanotube arrays. *RSC Adv.* 5, 10623–10631. doi:10.1039/c4ra14039g

## Conflict of interest

The authors declare that the research was conducted in the absence of any commercial or financial relationships that could be construed as a potential conflict of interest.

## Publisher's note

All claims expressed in this article are solely those of the authors and do not necessarily represent those of their affiliated organizations, or those of the publisher, the editors and the reviewers. Any product that may be evaluated in this article, or claim that may be made by its manufacturer, is not guaranteed or endorsed by the publisher.

## Supplementary material

The Supplementary Material for this article can be found online at: <https://www.frontiersin.org/articles/10.3389/fmats.2024.1407485/full#supplementary-material>

Hartanto, D., Yuhaneke, G., Utomo, W. P., Rozafia, A. I., Kusumawati, Y., Dahani, W., et al. (2022). Unveiling the charge transfer behavior within ZSM-5 and carbon nitride composites for enhanced photocatalytic degradation of methylene blue. *RSC Adv.* 12, 5665–5676. doi:10.1039/d1ra09406h

Huang, Z., Feng, G., Zhou, K., Han, J., Shi, Z., He, C., et al. (2022). Manufacture of TiO<sub>2</sub> nanoparticles with high preparation efficiency and photocatalytic performance by controlling the parameters of pulsed laser ablation in liquid. *Opt. Express* 30, 20482–20500. doi:10.1364/oe.455658

Hui, K. C., Ang, W. L., and Sambudi, N. S. (2021). Nitrogen and bismuth-doped rice husk-derived carbon quantum dots for dye degradation and heavy metal removal. *J. Photochem. Photobiol. A Chem.* 418, 113411. doi:10.1016/j.jphotochem.2021.113411

Jin, S. H., Kim, D. H., Jun, G. H., Hong, S. H., and Jeon, S. (2013). Tuning the photoluminescence of graphene quantum dots through the charge transfer effect of functional groups. *ACS nano* 7, 1239–1245. doi:10.1021/nn304675g

Karimifard, S., and Moghaddam, M. R. A. (2018). Application of response surface methodology in physicochemical removal of dyes from wastewater: a critical review. *Sci. Total Environ.* 640, 772–797. doi:10.1016/j.scitotenv.2018.05.355

Katheresan, V., Kansedo, J., and Lau, S. Y. (2018). Efficiency of various recent wastewater dye removal methods: a review. *J. Environ. Chem. Eng.* 6, 4676–4697. doi:10.1016/j.jece.2018.06.060

Kumar, S., Dhiman, A., Sudhagar, P., and Krishnan, V. (2018). ZnO-graphene quantum dots heterojunctions for natural sunlight-driven photocatalytic environmental remediation. *Appl. Surf. Sci.* 447, 802–815. doi:10.1016/j.apsusc.2018.04.045

Laghari, A. J., Aftab, U., Tahira, A., Shah, A. A., Gradone, A., Solangi, M. Y., et al. (2023). MgO as promoter for electrocatalytic activities of Co<sub>3</sub>O<sub>4</sub>-MgO composite via abundant oxygen vacancies and Co<sup>2+</sup> ions towards oxygen evolution reaction. *Int. J. Hydrogen Energy* 48, 12672–12682. doi:10.1016/j.ijhydene.2022.04.169

Marszewski, M., Marszewska, J., Pylypenko, S., and Jaromic, M. (2016). Synthesis of porous crystalline doped titania photocatalysts using modified precursor strategy. *Chem. Mater.* 28, 7878–7888. doi:10.1021/acs.chemmater.6b03429

Molla, M. A. I., Tateishi, I., Furukawa, M., Katsumata, H., Suzuki, T., and Kaneco, S. (2017). Evaluation of reaction mechanism for photocatalytic degradation of dye with self-sensitized TiO<sub>2</sub> under visible light irradiation. *Open J. Inorg. non-metallic Mater.* 7, 1–7. doi:10.4236/ojinn.2017.71001

Mondol, B., Sarker, A., Shareque, A. M., Dey, S. C., Islam, M. T., Das, A. K., et al. (2021). Preparation of activated carbon/TiO<sub>2</sub> nanohybrids for photodegradation of reactive red-35 dye using sunlight. *Photochem* 1, 54–66. doi:10.3390/photochem1010006

- Nasir, J. A., ur Rehman, Z., Shah, S. N. A., Khan, A., Butler, I. S., and Catlow, C. R. A. (2020). Recent developments and perspectives in CdS-based photocatalysts for water splitting. *J. Mater. Chem. A* 8 (40), 20752–20780. doi:10.1039/d0ta05834c
- Nizam, N. U. M., Hanafiah, M. M., Mahmoudi, E., and Mohammad, A. W. (2023). Synthesis of highly fluorescent carbon quantum dots from rubber seed shells for the adsorption and photocatalytic degradation of dyes. *Sci. Rep.* 13, 12777. doi:10.1038/s41598-023-40069-w
- Nugraha, M. W., Abidin, N. H. Z., and Sambudi, N. S. (2021). Synthesis of tungsten oxide/amino-functionalized sugarcane bagasse derived-carbon quantum dots (WO<sub>3</sub>/N-CQDs) composites for methylene blue removal. *Chemosphere* 277, 130300. doi:10.1016/j.chemosphere.2021.130300
- Olak-Kucharczyk, M., Szczepańska, G., Kudzin, M. H., and Pisarek, M. (2020). The photocatalytic properties of RGO/TiO<sub>2</sub> coated fabrics. *Coatings* 10, 1041. doi:10.3390/coatings10111041
- Pan, D., Jiao, J., Li, Z., Guo, Y., Feng, C., Liu, Y., et al. (2015). Efficient separation of electron-hole pairs in graphene quantum dots by TiO<sub>2</sub> heterojunctions for dye degradation. *ACS Sustain. Chem. Eng.* 3, 2405–2413. doi:10.1021/acssuschemeng.5b00771
- Pan, D., Zhang, J., Li, Z., and Wu, M. (2010). Hydrothermal route for cutting graphene sheets into blue-luminescent graphene quantum dots. *Adv. Mater.* 22, 734–738. doi:10.1002/adma.200902825
- Panagopoulos, A. (2022a). Brine management (saline water and wastewater effluents): sustainable utilization and resource recovery strategy through Minimal and Zero Liquid Discharge (MLD and ZLD) desalination systems. *Chem. Eng. Processing-Process Intensif.* 176, 108944. doi:10.1016/j.ccep.2022.108944
- Panagopoulos, A. (2022b). Techno-economic assessment and feasibility study of a zero liquid discharge (ZLD) desalination hybrid system in the Eastern Mediterranean. *Chem. Eng. Processing-Process Intensif.* 178, 109029. doi:10.1016/j.ccep.2022.109029
- Panagopoulos, A., and Giannika, V. (2022). Decarbonized and circular brine management/valorization for water and valuable resource recovery via minimal/zero liquid discharge (MLD/ZLD) strategies. *J. Environ. Manag.* 324, 116239. doi:10.1016/j.jenvman.2022.116239
- Peng, H., and Guo, J. (2020). Removal of chromium from wastewater by membrane filtration, chemical precipitation, ion exchange, adsorption electrocoagulation, electrochemical reduction, electro dialysis, electrodeionization, photocatalysis and nanotechnology: a review. *Environ. Chem. Lett.* 18, 2055–2068. doi:10.1007/s10311-020-01058-x
- Qin, J., Zhang, X., Yang, C., Cao, M., Ma, M., and Liu, R. (2017). ZnO microspheres-reduced graphene oxide nanocomposite for photocatalytic degradation of methylene blue dye. *Appl. Surf. Sci.* 392, 196–203. doi:10.1016/j.apsusc.2016.09.043
- Rajabi, H. R., Arjmand, H., Kazemdehdashti, H., and Farsi, M. (2016). A comparison investigation on photocatalytic activity performance and adsorption efficiency for the removal of cationic dye: quantum dots vs. magnetic nanoparticles. *J. Environ. Chem. Eng.* 4, 2830–2840. doi:10.1016/j.jece.2016.05.029
- Rezaei, B., Irannejad, N., Ensafi, A. A., and Kazemifard, N. (2019). The impressive effect of eco-friendly carbon dots on improving the performance of dye-sensitized solar cells. *Sol. Energy* 182, 412–419. doi:10.1016/j.solener.2019.02.072
- Roza, L., Fauzia, V., Rahman, M. Y. A., Isnaeni, I., and Putro, P. A. (2020). ZnO nanorods decorated with carbon nanodots and its metal doping as efficient photocatalyst for degradation of methyl blue solution. *Opt. Mater.* 109, 110360. doi:10.1016/j.optmat.2020.110360
- Rusmin, R., Sarkar, B., Mukhopadhyay, R., Tsuzuki, T., Liu, Y., and Naidu, R. (2022). Facile one pot preparation of magnetic chitosan-palygorskite nanocomposite for efficient removal of lead from water. *J. Colloid Interface Sci.* 608, 575–587. doi:10.1016/j.jcis.2021.09.109
- Sabet, M., and Mahdavi, K. (2019). Green synthesis of high photoluminescence nitrogen-doped carbon quantum dots from grass via a simple hydrothermal method for removing organic and inorganic water pollution. *Appl. Surf. Sci.* 463, 283–291. doi:10.1016/j.apsusc.2018.08.223
- Sajjadi, S., Khataee, A., and Kamali, M. (2017). Sonocatalytic degradation of methylene blue by a novel graphene quantum dots anchored CdSe nanocatalyst. *Ultrason. Sonochemistry* 39, 676–685. doi:10.1016/j.ultsonch.2017.05.030
- Sajjadi, S., Khataee, A., Soltani, R. D. C., and Hasanzadeh, A. (2019). N, S co-doped graphene quantum dot-decorated Fe<sub>3</sub>O<sub>4</sub> nanostructures: preparation, characterization and catalytic activity. *J. Phys. Chem. Solids* 127, 140–150. doi:10.1016/j.jpcs.2018.12.014
- Shahib, I. I., Iftikhar, J., Oyekunle, D. T., Elkhilfi, Z., Jawad, A., Wang, J., et al. (2022). Influences of chemical treatment on sludge derived biochar; physicochemical properties and potential sorption mechanisms of lead (II) and methylene blue. *J. Environ. Chem. Eng.* 10, 107725. doi:10.1016/j.jece.2022.107725
- Shelar, S. G., Mahajan, V. K., Patil, S. P., and Sonawane, G. H. (2020). Effect of doping parameters on photocatalytic degradation of methylene blue using Ag doped ZnO nanocatalyst. *SN Appl. Sci.* 2, 820. doi:10.1007/s42452-020-2634-2
- Sudhaik, A., Raizada, P., Shandilya, P., Jeong, D. Y., Lim, J. H., and Singh, P. (2018). Review on fabrication of graphitic carbon nitride based efficient nanocomposites for photodegradation of aqueous phase organic pollutants. *J. Industrial Eng. Chem.* 67, 28–51. doi:10.1016/j.jiec.2018.07.007
- Sugarti, S., and Darmawan, N. (2015). Synthesis of fluorescence carbon nanoparticles from ascorbic acid. *Indonesian J. Chem.* 15 (2), 141–145. doi:10.1016/j.jic.212107
- Sun, C., Xu, Q., Xie, Y., Ling, Y., Jiao, J., Zhu, H., et al. (2017). High-efficient one-pot synthesis of carbon quantum dots decorating Bi<sub>2</sub>MoO<sub>6</sub> nanosheets heterostructure with enhanced visible-light photocatalytic properties. *J. Alloys Compd.* 723, 333–344. doi:10.1016/j.jallcom.2017.06.130
- Tetsuka, H., Asahi, R., Nagoya, A., Okamoto, K., Tajima, I., Ohta, R., et al. (2012). Optically tunable amino-functionalized graphene quantum dots. *Adv. Mater. Deferf. Beach, Fla.* 24, 5333–5338. doi:10.1002/adma.201201930
- Velasco, L. F., Maurino, V., Laurenti, E., and Ania, C. (2013). Light-induced generation of radicals on semiconductor-free carbon photocatalysts. *Appl. Catal. A General* 453, 310–315. doi:10.1016/j.apcata.2012.12.033
- Velumani, A., Sengodan, P., Arumugam, P., Rajendran, R., Santhanam, S., and Palanisamy, M. (2020). Carbon quantum dots supported ZnO sphere based photocatalyst for dye degradation application. *Curr. Appl. Phys.* 20, 1176–1184. doi:10.1016/j.cap.2020.07.016
- Yang, C., Zhang, X., Qin, J., Shen, X., Yu, R., Ma, M., et al. (2017). Porous carbon-doped TiO<sub>2</sub> on TiC nanostructures for enhanced photocatalytic hydrogen production under visible light. *J. Catal.* 347, 36–44. doi:10.1016/j.jcat.2016.11.041
- Yang, W., Tang, S., Wei, Z., Chen, X., Ma, C., Duan, J., et al. (2021). Separate-free BiPO<sub>4</sub>/graphene aerogel with 3D network structure for efficient photocatalytic mineralization by adsorption enrichment and photocatalytic degradation. *Chem. Eng. J.* 421, 129720. doi:10.1016/j.ccej.2021.129720
- Yang, Y., Cui, J., Zheng, M., Hu, C., Tan, S., Xiao, Y., et al. (2012). One-step synthesis of amino-functionalized fluorescent carbon nanoparticles by hydrothermal carbonization of chitosan. *Chem. Commun.* 48, 380–382. doi:10.1039/c1cc15678k
- Yu, B. Y., and Kwak, S. Y. (2012). Carbon quantum dots embedded with mesoporous hematite nanospheres as efficient visible light-active photocatalysts. *J. Mater. Chem.* 22 (17), 8345–8353. doi:10.1039/c2jm16931b
- Yu, H., Zhang, B., Bulin, C., Li, R., and Xing, R. (2016). High-efficient synthesis of graphene oxide based on improved hummers method. *Sci. Rep.* 6, 36143–36147. doi:10.1038/srep36143
- Zhang, J., Zhang, X., Dong, S., Zhou, X., and Dong, S. (2016). N-doped carbon quantum dots/TiO<sub>2</sub> hybrid composites with enhanced visible light driven photocatalytic activity toward dye wastewater degradation and mechanism insight. *J. Photochem. Photobiol. A Chem.* 325, 104–110. doi:10.1016/j.jphotochem.2016.04.012
- Zhang, Z., Sun, W., and Wu, P. (2015). Highly photoluminescent carbon dots derived from egg white: facile and green synthesis, photoluminescence properties, and multiple applications. *ACS Sustain. Chem. Eng.* 3, 1412–1418. doi:10.1021/acssuschemeng.5b00156
- Zhang, Z., Zheng, T., Li, X., Xu, J., and Zeng, H. (2016). Progress of carbon quantum dots in photocatalysis applications. *Part. Part. Syst. Charact.* 33, 457–472. doi:10.1002/ppsc.201500243
- Zhao, Y., Liu, L., Cui, T., Tong, G., and Wu, W. (2017). Enhanced photocatalytic properties of ZnO/reduced graphene oxide sheets (rGO) composites with controllable morphology and composition. *Appl. Surf. Sci.* 412, 58–68. doi:10.1016/j.apsusc.2017.03.207
- Zheng, M., Xie, Z., Qu, D., Li, D., Du, P., Jing, X., et al. (2013). On-off-on fluorescent carbon dot nanospheres for recognition of chromium (VI) and ascorbic acid based on the inner filter effect. *ACS Appl. Mater. Interfaces* 5, 13242–13247. doi:10.1021/am4042355
- Zhu, L., Shen, D., Liu, Q., Luo, K. H., and Li, C. (2022). Mild acidolysis-assisted hydrothermal carbonization of lignin for simultaneous preparation of green and blue fluorescent carbon quantum dots. *ACS Sustain. Chem. Eng.* 10, 9888–9898. doi:10.1021/acssuschemeng.2c02223